Glucose Concentration Measurement Using Homodyne I/Q Interferometer

Sovannarith Hut[1,2], Sreyleak Ean[1], Lim Lorn[3], Saren Vy[3], Sophat Houn[3], and Seang Hor Eang[3,*]

ARTICLE INFO

Article history:
Received: 9 March 2024
Revised: 10 May 2024
Accepted: 8 June 2024
Online: 30 June 2025

Keywords:
Glucose concentration
Homodyne I/Q
Interferometer
Microfluidic channel

ABSTRACT

Glucose, sourced from metabolized carbohydrates, functions as the primary energy source in the human body. Its crucial role in cellular metabolism ensures the effective operation of various physiological processes. Moreover, glucose levels serve as an essential diagnostic indicator for diabetes, enabling healthcare professionals to evaluate an individual's glycemic control and overall health. Consequently, there is a need for highly sensitive, accurate, and stable glucose measurement devices or technologies. The balanced-path homodyne I/Q-interferometer has been utilized in numerous applications as a readout sensor for chemical concentrations in various solutions. In our study, we employed the balanced-path homodyne I/Q-interferometer to measure standard glucose solutions prepared at concentrations of 10^{-1} M, 10^{-2} M, 10^{-3} M, and 10^{-4} M. This analysis resulted in deriving a linear equation of the form $y = (610.98089 \pm 7.509)x + (0.84751 \pm 0.37736)$ with an impressive R-squared value of 0.9997. In this equation, y denotes the phase change of glucose and deionized water in radians (rad), while x represents the concentration of glucose in millimolar (mM). Utilizing this equation, we can determine the concentration of any glucose solution in the experimental setup when the glucose concentration is unknown. By inputting the value of the phase change in radians (y) into the linear equation, we can identify the concentration of the unknown glucose solution. This research offers significant potential for society by enhancing the detection of glucose concentration in solutions with high sensitivity. Moreover, it presents a promising technique for glucose concentration sensors, particularly in the medical field, where precise measurements play a crucial role, especially for individuals with diabetes.

1. INTRODUCTION

Glucose is a simple sugar with the chemical formula $C_6H_{12}O_6$, a monosaccharide containing an aldehyde group (-CHO) [1]. It is the primary energy source derived from metabolic carbohydrates. It serves as an indicator for assessing human health, particularly in the context of diabetes [2]. In 2019, the total number of people with diabetes was reported to be 463 million, and this figure is projected to increase to 507 million by 2030 [3]. As the number of patients grows, there is a growing need for highly sensitive, accurate, and stable glucose measurement devices or technologies in healthcare.

The concentration of glucose can be measured using a variety of techniques, including enzymatic and electrochemical approaches [4]. However, the slow progress of glucose electro-oxidation on electrodes restricts the sensitivity of the electrochemical approach [5]. Even with the increased sensitivity of the enzymatic approach, there are still issues related to the intricate immobilization procedure [6].

Two-beam interferometry, whether heterodyne or homodyne, has found extensive application in precision optical sensor systems due to its remarkably high sensitivity [7]. The homodyne in-phase and quadrature (I/Q) interferometry, which consists of a single-frequency laser source and a homodyne detector, is commonly employed to enhance sensitivity [8]. The system has implemented a stabilized laser to achieve this. The scanning balanced-path homodyne I/Q-interferometer is applied in some application sensors. Through signal processing, the system can be measured at low frequencies or baseband. The homodyne I/Q detector has been used for acquiring separate and simultaneous measurement of amplitude and phase modulation without requiring calibrations [9,10]. Many useful applications of two beams such as: scanning microscopy, displacement sensor, biosensor, surface topography, electronic fabrication, chemical readout sensor

[1]*Faculty of Electricity, National Polytechnic Institute of Cambodia, Phnom Penh, 120901, Cambodia.*
[2]*Graduate School, National Polytechnic Institute of Cambodia, Phnom Penh,120901, Cambodia.*
[3]*Graduate School of Science, Royal University of Phnom Penh, Phnom Penh, Cambodia*.
**Corresponding author:* Seang Hor Eang; Phone: +855-61-302-017; Email: eang.seanghor@rupp.edu.kh.

and so forth, [11–18]. The homodyne I/Q-interferometer has been applied for many applications such as chemical concentration readout sensor, displacement sensors, biochip imaging, optical scanning microscope and other important applications can be found [10,11].

From the extensive body of previous research, it is observed that interferometry has been employed to measure the chemical concentrations of various solutions. Jeong et al. introduced the scanning interferometer as a multiport interferometer used to map the variation of magnitude and phase of complex reflection coefficients of the surface or thin film, and also to identify and locate defects on the surface [19]. June Gyu et al. proposed a high-precision tilt measurement using a folded Mach-Zehnder geometry in-phase. This high-sensitivity homodyne interferometer can measure the phase change induced by in-plane tilt of the target (tilt mirror in this case), while remaining insensitive to other target motions [15]. Furthermore, Eang et al. proposed the scanning balanced-path homodyne I/Q interferometer scheme for obtaining phase and amplitude images of protein biochip samples prepared using the sandwich Enzyme-Linked Immunosorbent Assay (ELISA) technique [9]. Yoon et al. proposed a balanced-path heterodyne I/Q-interferometer system, which was successfully applied to measure refractive indexes of sodium chloride, ethylene glycol, and ethyl alcohol solutions. In their study, the minimum detectable concentration of ethylene glycol solution was determined to be 0.003 wt% and the change in refractive index (Δn) was determined to be 2.3×10^{-8}, corresponding to a concentration of 2.07×10^{-5} vol% [10]. It is worth noting that the sensitivity could potentially be enhanced through the improvement of the fluidic channel design [10,20].

In this research, we will utilize a homodyne I/Q-interferometer with a balanced-path configuration, where the optical path length between the probe beam (PB) and reference beam (RB) is kept the same. By utilizing the balanced-path scheme, our interferometer can effectively reject various noises such as temperature turbulence, environmental vibration, and interference from the sample path between the beams. It has the capability to measure both the phase and amplitude changes induced on the PB, as well as the phase difference between the PB and RB, without requiring any calibration procedures [11]. The experiment will utilize standard glucose solutions with different concentrations of 10^{-1} M, 10^{-2} M, 10^{-3} M and 10^{-4} M. These solutions were carefully prepared in the Chemistry Laboratory of the Royal University of Phnom Penh and measured in molar concentrations. The concentration of glucose will be determined using a microfluidic channel. The measurement results will be fitted with a linear function in order to determine the standard curve [21].

2. EXPERIMENTAL SETUP

2.1. Structural design and experimental procedure

A He-Ne laser, specifically the Thorlabs HRS015B model, operates with a wavelength of 632.992 nm. This laser is meticulously stabilized to a single frequency and serves as the input beam. The input beam is rotated by 45 degrees using an optical isolator (OI). The output beam from the OI, with a polarization plane at 45 degrees, is split into two perpendicular directions after passing through the polarizing beam splitter (PBS1): The transmitted beam is used as PB and the reflected beam is used as RB, respectively. The PB is represented by a solid line and the RB is represented by a dashed line as shown in Fig. 1. The PB travels straight and is reflected by prism1 before being directed through the microfluidic channel system. The reflection of PB from the microfluidic channel passes through QWP2 twice, resulting in a 90-degree rotation of the optical beam's polarization plane. The PB is then reflected at a right angle from PBS1, passes through QWP3, is reflected back by Prism2, before passing through PBS1 to QWP1. Similar to QWP2, the PB undergoes a 90-degree rotation of the optical beam's polarization. The beam reflected back from the mirror-coated QWP1 was then redirected at PBS1 and sent into the homodyne I/Q-demodulator by being reflected from prism3, as depicted in the annotated area of Fig. 1.

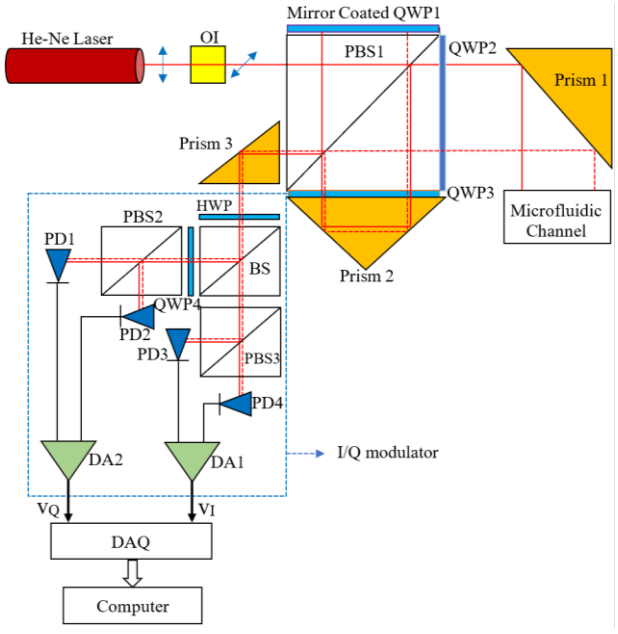

Fig. 1. Schematic diagram of glucose concentration readout sensor.

In other words, The RB is directed to the mirror-coated QWP1. Once reflected, the RB is transmitted at PBS1 and then guided to a right-angle prism. This process continues as the returned PB travels back and forth between the right prism, PBS1, and the channel for scanning. Eventually, the RB is sent to the homodyne I/Q demodulator after passing through these components. Both the PB and RB follow the same optical path length with minimal beam separation, making them relatively immune to environmental noise. As

illustrated in Fig.1, the compact and small size of the optical components used in this experimental setup is evident, as PBS1, mirror-coated QWP1, QWP2, QWP3, and the prism are all securely connected. The PB and RB construct an interference pattern and are investigated by an optical sensor as an I/Q-homodyne detector.

In the I/Q demodulator, both the PB and RB undergo a 45-degree rotation by the half-wave plate (HWP), aligning the fast axis with respect to the horizontal axis. They are then both transmitted and reflected by a beam splitter (BS). Following this, the transmitted beam containing PB and RB information is further reflected and transmitted by PBS3. Information from the reflected beam and the transmitted beam is extracted by photodiode 3 (PD3) and photodiode 4 (PD4) respectively. Subsequently, the signals from PD3 and PD4 are fed into the differential amplifier 1 (DA1), resulting in the in-phase quadrature signal denoted as V_I.

Simultaneously, both the PB and RB are reflected at the BS, passing through quarter-wave plate 4 (QWP4), and then combined at PBS2. QWP4 is set at a 45-degree angle to both PB and RB, purposefully introducing a 90-degree phase difference between the RB and PB. Information from the PB and RB components is extracted by photodiode 1 (PD1) and photodiode 2 (PD2) respectively. Both PD1 and PD2 are connected to differential amplifier 2 (DA2). The output signal from DA2, referred to as the quadrature signal, is denoted as V_Q. By utilizing the I/Q-demodulation technique, the changing phase and amplitude of the PB and RB are concurrently and distinctly obtained from the provided equations.

The signals derived from PD1 and PD2 will be identified as the quadrature-phase signal.

$$v_Q = R|E_{PB}||E_{RB}|\sin(\Delta\phi) \quad (1)$$

The signals obtained from PD3 and PD4 will be labeled as the in-phase signal.

$$v_I = R|E_{PB}||E_{RB}|cos(\Delta\phi) \quad (2)$$

From equations (1) and (2), we obtain the phase on the PB:

$$\Delta\phi = tan^{-1}\left(\frac{v_Q}{v_I}\right) \quad (3)$$

The change in phase when measuring glucose solution and DI water, with respect to the change in refractive index, is denoted by equations (4)[22],

$$\Delta\phi = \frac{4\pi l\Delta n}{\lambda} \quad (4)$$

where, $\Delta\phi$ corresponds to the phase change induced by glucose and deionized (DI) water. Δn represents the change in refractive index between the sample and DI water, λ denotes the wavelength of the light source and l is the depth of the channel. In Equation (4), it is indicated that theoretical phase difference is a linear function of the refractive index change in the sample and DI water. Consequently, the phase difference must also exhibit a linear relationship with the glucose concentration [21].

2.2. Microfluidic channel system design

A microfluidic channel system resembles a small-scale plumbing network designed to transport liquids or solutions through tiny channels. Imagine it as a miniaturized arrangement of pipes and channels that can precisely control and manipulate fluid flow at the microscale. This technology finds applications in diverse fields such as biology, chemistry, and engineering. Essentially, it provides a sophisticated and precise method for handling small liquid volumes across various practical contexts [23].

For our design, we established a configuration consisting of three layers of microfluidic channels, each featuring a cross-sectional area of 5 cm by 5 cm. To enhance functionality, the inner surfaces of these channels have been coated with a reflective finish. The initial layer has been meticulously crafted as a 3 mm thick mirrored rectangle, while the subsequent layer mirrors both its size and shape, fashioned from a 1 mm thick glass plate. The ultimate layer is enveloped in glass possessing properties similar to those of the second layer. Notably, an adaptation was introduced by perforating the glass plate layer to create a parallel rectangular configuration with a 2 mm by 2 mm cross-sectional area. This alteration facilitates the passage of glucose solutions as a sample, alongside DI water for reference purposes. The microfluidic channel system consists of a single channel called the probe channel (PCH). The PCH is used for the movement of glucose concentration flow, which serves as the sample, while DI water acts as the reference flow. The flow into and out of the channel is governed by gravity, with a variance in height of 7 cm during the process. The PB is directed straight onto the PCH, while the RB is aimed at the mirror, as explained in Fig. 2.

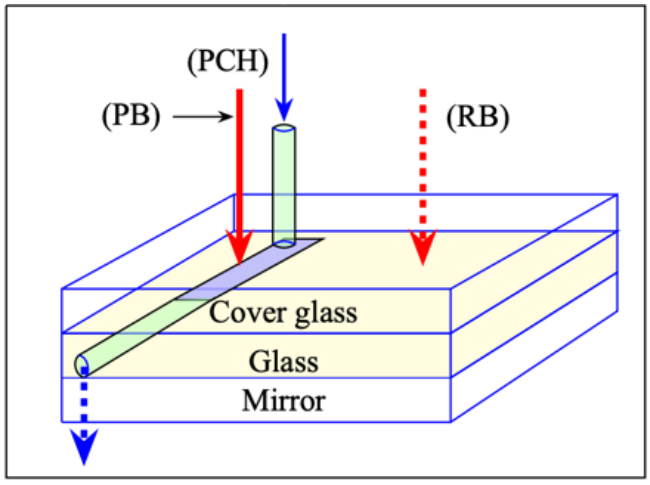

Fig. 2. The microfluidic channel system design.

3. RESULTS AND DISCUSSION

In our I/Q-homodyne interferometer setup, we analyze fluidic channel through which both a sample and a reference fluid flow. For our experiment, we employed a custom-made single microfluidic channel to measure various concentrations of glucose solutions. These standard glucose solutions were meticulously prepared at concentrations of 10^{-1} M, 10^{-2} M, 10^{-3} M, and 10^{-4} M. As our reference liquid, we used DI water, also known as distilled water. DI water serves as a baseline for comparison in various scientific measurements, including refractive index determination. By establishing the refractive index of the reference liquid (in this case, DI water), we can then compare it to the refractive index of our glucose solution sample. This comparison allows us to calculate the phase difference, which ultimately enables us to determine the glucose concentration. The phase shift experienced is influenced by the solute present and its concentration as the reference and sample liquids alternate their flow through the channel, modulating the phase of the PB. The flow of solutions in and out of the channel is influenced by gravity, which occurs due to a 7 cm height disparity. For instance, in Fig. 3(a), we employed the standard glucose concentration of 10^{-1} M to measure the phase change within our experimental setup. Initially, the valve was opened to allow DI water to flow through the channel for a duration of 3 minutes. Subsequently, the DI water valve was closed, and the flow of the glucose solution commenced at 3.5 minutes along the microfluidic channel. The signal underwent a rapid phase transition from 0 radians to 62 radians before stabilizing. Following this, the glucose solution valve was turned off, and the valve was switched back to DI water between the 10-minute and 15-minute marks. Consequently, the signal reverted to a phase change value of zero, mirroring the initial phase change observed with DI water over a 3-minute period. This outcome signifies that for a glucose concentration of 10^{-1} M, the phase disparity between glucose and DI water amounts to 62 radians. The experimental process persisted in a comparable manner for the remaining glucose solutions, adhering to the same methodology as that of the 10^{-1} M glucose solution. Upon scrutinizing the outcomes for varying glucose concentrations in Fig. 3(b), it is evident that at a concentration of 10^{-2} M, an angular displacement of 6.35 radians was noted. Furthermore, in Fig. 3(c), a concentration of 10^{-3} M resulted in a phase shift of 2.1 radians, and lastly, in Fig. 3(d), the concentration of 10^{-4} M yielded a phase shift of 0.82 radians.

Consequently, increasing glucose concentrations result in a proportional rise in phase change. When examining glucose concentrations, the measurement outcomes are represented as a linear relationship between concentration and phase shift, demonstrated in Fig. 4. These results were fitted with a linear equation ($R^2 = 0.9997$), yielding the standard curve $y = (610.98089 \pm 7.509)x + (0.84751 \pm 0.37736)$, where y represents the phase change of glucose and DI water in radians (rad), and x represents the concentration of glucose in millimolar (mM).

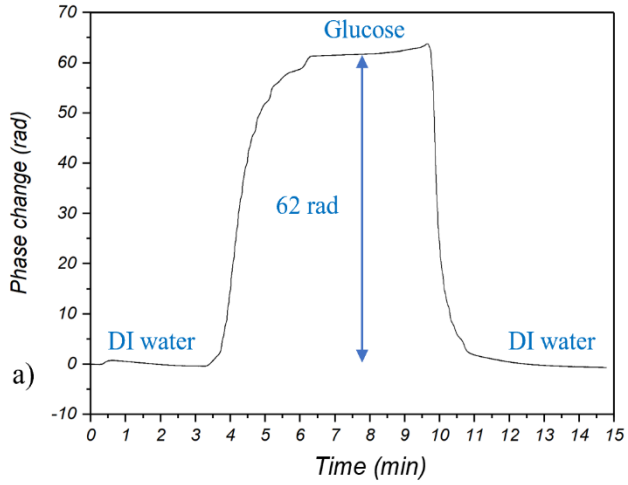

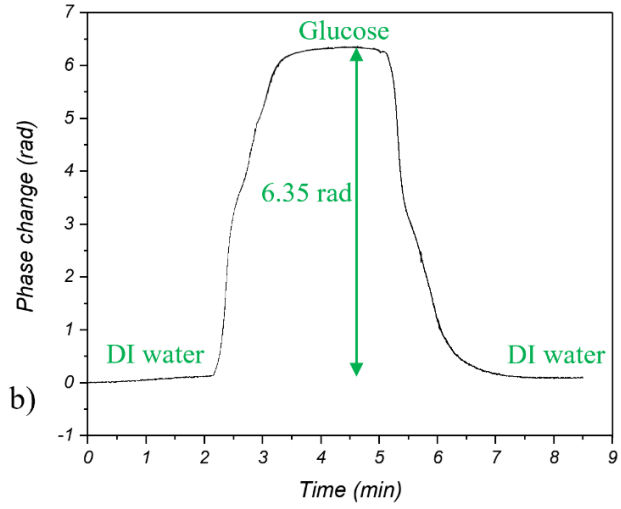

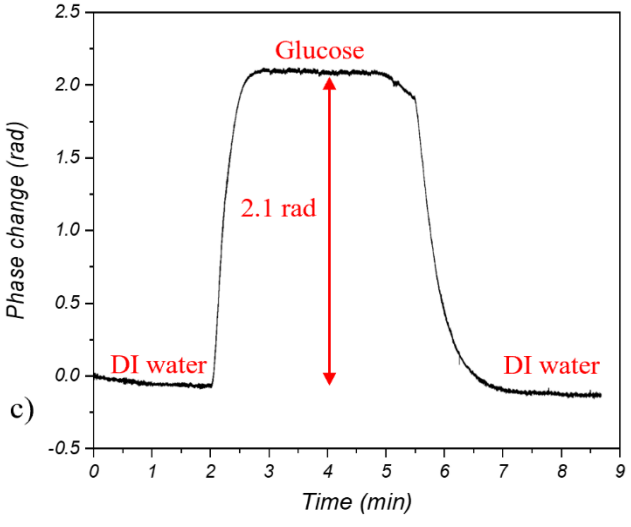

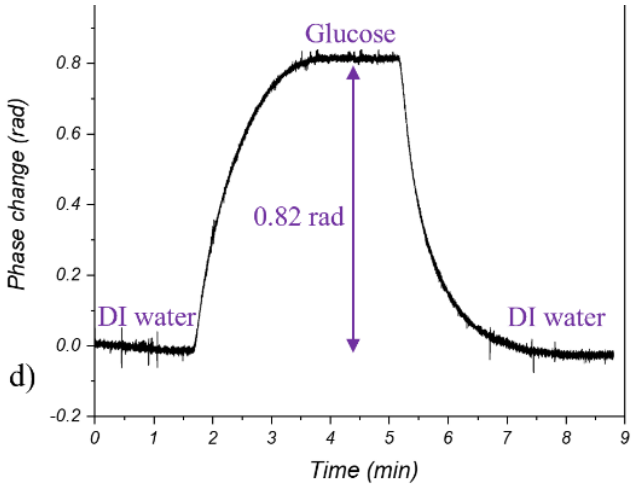

Fig. 3. The experimental results of phase change of glucose concentration by using balanced-path homodyne I/Q-interferometer. (a). 10^{-1} M, (b). 10^{-2} M, (c). 10^{-3} M, (d). 10^{-4} M.

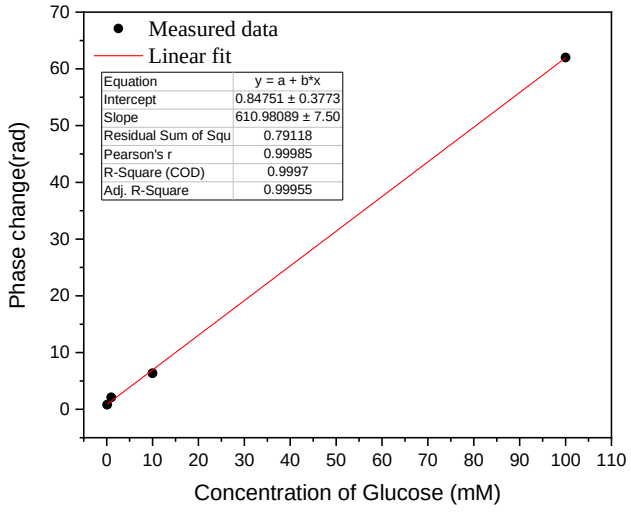

Fig. 4. The linear curve fitting of the phase change and standard glucose concentration.

4. CONCLUSIONS

The balanced-path homodyne I/Q-interferometer is applied to measure glucose concentration, which is a highly sensitive, accurate, and stable glucose measurement device or technology. By using standard glucose solutions at concentrations of 10^{-1} M, 10^{-2} M, 10^{-3} M, and 10^{-4} M, we obtained a linear equation of the form y = (610.98089 ± 7.509) x + (0.84751 ± 0.37736), where (y) represents the phase change of glucose and DI water in radians (rad), while (x) corresponds to the concentration of glucose in millimolar (mM). The high goodness-of-fit (R-squared value of 0.9997) validates the reliability of our model. From this equation, we can calculate the concentration of other glucose solutions by leveraging the phase difference observed in our experimental setup. This research holds significant potential for society by aiding in the detection of glucose concentration in solutions with high sensitivity. Moreover, it represents another promising technique for glucose concentration sensors, particularly in the context of medical needs, especially for diabetics.

ACKNOWLEDGEMENTS

This work was supported by National Polytechnic Institute of Cambodia and Higher Education Improvement Project (HEIP) funded by the Royal Government of Cambodian (IDA Credit No. 6221-KH) through Ministry of Education, Youth and Sport, and Sweden-RUPP Bilateral Programme (Sida Contribution No. 11599).

REFERENCES

[1] Shendurse, A.M. (2016). Encyclopedia of Food and Health || Glucose: Properties and Analysis.239–47. doi:10.1016/b978-0-12-384947-2.00353-6.

[2] Jessica, L.H.; Meda, E. P.; Dianna, J.M.; Jonathan, E. S.; Edward, W.G. 2028. Global trends in diabetes complications: a review of current evidence. Diabetologia. 62(1): 3-16.doi: 10.1007/s00125-018-4711-2

[3] Pouya, S.; Inga, P.; Paraskevi, S.; Belma, M.; Suvi, K.; Nigel, U.; Stephen, C.; Leonor, G.; Ayesha, A. M.; Katherine, O.; Jonathan, E.S.; Dominic, B.; Rhys, W.; et al. 2019. Gobal and regional diabetes prevalence estimate for 2019 and projections for 2030 and 2045: Results from the international diabetes federation diabetes atlas, 9th edition. Diabetes Res. Clin. Pract. 157. 107843. doi: 10.1016/j.diabres.2019.107843.

[4] Hui-Chen, W.; Ang-Rong, L. 2015. Recent developments in blood glucose sensors. Journal of Food and drug Ana. 23(2): 191-200. doi.org/10.1016/j.jfda.2014.12.001

[5] Chao, C.; Qingji, X.; Dawei, Y.; Hualing, X.; Yingchun, F.; Yueming, T.; Shouzhuo, Y. 2013. Recent advances in electrochemical glucose biosensors: A review. RSC. Adv. 3(14): 4473-4491. doi:10.1039/C2RA22351A

[6] Danielle, B.; Colm, D.; Larisa, F.; Dermot, D. 2017. Glucose sensing for diabetes monitoring: Recent developments. Sensors (Basel). 17(8): 1866. doi: 10.3390/s17081866

[7] Guido, S.; Juan, S.F.C.; Ingo, O.; et al. 2021. A heterodyne interferometer with separated beam paths for high-precision displacement and angular measurement. Nano. and Met. 4(3): 1-8. doi: 10.1007/s41871-021-00101-x

[8] Cam, N.; Seoktae, K. 2011. RF homodyne interferometric sensor. Springer Briefs in Phys. doi: 10.1007/978-1-4614-2023-1_3

[9] Eang, S. H. 2014. Balanced-path Homodyne I/Q-interferometers and Their Application. Sogang Uni. Ph.D. thesis. 6 − 14

[10] Seunghyn, Y.; Youngkyu, P.; Kyuman, C. 2013. A new balanced-path heterodyne I/Q-interferometer scheme for low environmental noise, high sensitivity phase measurements for both reflection and transmission geometry. Opt. Express, 21(18), 20722 – 20729. doi:10.1364/OE.21.020722

[11] Eang, S. H.; Yoon, S.; Park, J. G.; Cho, K. 2015. Scanning balanced-path homodyne I/ Q-interferometer scheme and its applications. Opt. Express. 40(11): 2457 – 2460. doi.org/10.1364/OL.40.002457

[12] Hut, S.; Ean, S.; Eang, S. H.; Kim, Y. G. 2025. Mode

matching and lasing characteristic in end-pumped Nd:YAG laser. GMSARN Inter. Jour. 19(01): 78-85

[13] Wang, Z.; Zhang, L.; Wang, S.; Xue, N.; Peng, F.; Fan, M.; Sun, W.; Qian, X.; Rao, J.; Rao, Y. 2016. Coherent Φ-OTDR based on I/Q demodulation and homodyne detection. Opt. Express, 24(02): 853. doi:10.1364/OE.24.000853

[14] He, Z.; Cui, J.; Tan, J.; Bian, X.; Jiang, W. 2018. Discrete fringe phase unwrapping algorithm based on Kalman motion estimation for high speed I/Q-interferometry. Opt. Expres. 26(07): 8699 – 8708.doi:10.1364/OE.26.008699

[15] Park, J. G.; Cho, K. 2016. High-precision tilt sensor using a folded Mach–Zehnder geometry in-phase and quadrature interferometer. App. Opt.55(09):2155−2159.doi: 10.1364/ AO.55.002155.

[16] Cui, J.; Li, W.; Bian, X.; Zhu, G.; He, Z.; Zou, L. 2021. Undersampling homodyne I/Q interferometer for ultra-low-frequency vibration calibration. Opt. Com. 478.doi.org/ 10.1016/j.optcom.2020.126394

[17] Eang, S. H.; Cho, K. 2017. Balanced-path homodyne I/Q-interferometer scheme with very simple optical arrangement using a polarizing beam displacer. Opt. Exp.25(07): 8237-8244. doi: 10.1364/OE.25.008237

[18] Pan, Z.; Feng, J.;Hu, X.; Jia, C.; Huang, X. 2019. High sensitivity fiber sensor for measurement of Cd2+ concentration in aqueous solution based on reflective Mach-Zehnder interference with temperature calibration. Opt. Exp. 27(22) 32621-32629.doi: 10.1364/OE.27.032621

[19] Jeong, H.; Kim, J. H.; Cho, K. 2002. Complete mapping of complex reflection coefficient of a surface using a scanning homodyne multiport interferometer. Opt. Communication 204(1-6): 45 – 52. doi:10.1016/s0030-4018(02)01235-x

[20] Yoon, S.; Park, Y.; Choi, H. D.; Cho, K. 2011. High sensitivity readout sensor for a fluidic channel using an exactly balanced heterodyne interferometer. International Quantum Electronics Conference and Conference on Lasers and Electro-Optics Pacific Rim 2011. doi:10.1109/IQEC-CLEO.2011.6194142

[21] Yeh, Y.L. 2008. Real-time measurement of glucose concentration and average refractive index using a laser interferometer. Opt. and laser in Eng. 46(9):666-670. doi.org/10.1016/j.optlaseng.2008.04.008

[22] Kasap, S.O. 2001. Optoelectronics and photonics: principles and practices. New Jersy: Pearson, Prentice-Hall.178-179.

[23] Tan, J.N.; Alan, T.; Neild, A. 2013. Stability of flowing open fluidic channels. AIP Advances. 3(2):022121. doi:10.1063/1 .4792940